

# UC Davis

## UC Davis Previously Published Works

### Title

Porous organosilicates low-dielectric films for high-frequency devices

### Permalink

<https://escholarship.org/uc/item/6p75732s>

### Journal

Journal of Electronic Materials, 33(2)

### ISSN

0361-5235

### Authors

Knoesen, A  
Song, G  
Volksen, W  
[et al.](#)

### Publication Date

2004-02-01

Peer reviewed

# Porous Organosilicates Low-Dielectric Films for High-Frequency Devices

ANDRÉ KNOESEN,<sup>1,3</sup> GE SONG,<sup>1</sup> WILLI VOLKSEN,<sup>2</sup> ELBERT HUANG,<sup>2</sup>  
TEDDIE MAGBITANG,<sup>2</sup> LINDA SUNDBERG, JAMES L. HEDRICK,<sup>2</sup>  
CRAIG J. HAWKER,<sup>2</sup> and ROBERT D. MILLER<sup>2</sup>

1.—Electrical and Computer Engineering, University of California, Davis, CA 95616. 2.—IBM Almaden Research Center, San Jose, CA 95120. 3.—E-mail: knoesen@ece.ucdavis.edu

The dielectric properties are reported for nanoporous thin films of poly(methyl silsesquioxane) (MSSQ) for use as an ultralow, dielectric intermetal insulator. Direct experimental conformation is provided that the films have low dielectric constants with low loss up to 10 GHz. Low-frequency measurements are also reported.

**Key words:** Dielectric films, dielectric measurements, nanoporous films, permittivity measurement, transmission line measurements

## INTRODUCTION

The performance of integrated circuits improves by reducing the feature sizes to obtain smaller transistors with reduced gate delay that makes it possible for transistors to work in the microwave frequency range. However, as dimensions are scaled to the sub-micrometer region, the time for signals to propagate between devices, known as interconnect or resistance-capacitance (RC) delay, becomes the dominant effect and can eliminate the benefits of higher density, smaller devices. The RC delay increases with a decrease in wiring dimensions and pitch unless the metal resistivity or the dielectric constant of the insulating media decrease. Ideally, both should decrease to optimize performance. Copper interconnects are now preferred over aluminum because copper has roughly 40% lower metal interconnect resistivity.<sup>1,2</sup> To fully realize the benefits of copper interconnect technology, the thin-film insulator at the wiring level must have a dielectric constant much less than silicon dioxide. A lower dielectric-constant intermetal dielectric (IMD) serves also to improve power consumption and reduce crosstalk. In this paper, we report on the dielectric properties of a porous organosilicate developed for use as an IMD.

An IMD must satisfy many material and processing requirements besides having a low dielectric constant: (1) the dielectric properties must be

isotropic, (2) the film must show a low leakage current and must have a high breakdown voltage, (3) it must show low moisture absorption because during processing it will be in contact with several liquids including water, (4) the film must be thermally stable and withstand temperatures as high as 450°C, and (5) the film must be mechanically robust to survive chemical-mechanical polishing, which is used for planarization of copper metallurgy. A general interest exists in porous materials that meet these requirements. In such a material, the pore sizes need to be significantly smaller than the smallest feature size (e.g., 10%), the pore size distribution must be narrow to maintain good uniformity of the electrical and mechanical properties, and the pores ideally should not be interconnected to limit moisture absorption and environmental contamination. The absorption of water in the porous materials is of particular concern because of its high dielectric constant and losses in the microwave frequency regime. Water absorption, in particular, makes untreated porous silica, prepared by sol-gel methods, unattractive.<sup>3</sup>

We present results on nanoporous thin films of poly(methyl silsesquioxane) (MSSQ) that are prepared from organic/inorganic polymer hybrids using a sacrificial porogen approach. The MSSQ is prepared by hydrolysis of suitable trifunctional methyl silane derivatives ( $\text{RSiO}_{1.5}$ )<sub>n</sub> and has O-Si-O linkages that have a chemical behavior similar to silicon dioxide.<sup>4</sup> In MSSQ structures, each silicon atom is

(Received March 17, 2003; accepted August 18, 2003)

attached to three oxygen atoms and one carbon atom. The SSQ derivatives prepared by the hydrolysis of  $\text{RSiX}_3$  derivatives ( $\text{R}$  = alkyl, aryl;  $\text{X}$  = halogen, alkoxy) are selected as matrix materials for a number of reasons. After curing, they are chemically unreactive and exceptionally thermally stable. In the prepolymer, prior to curing, the end groups carry hydroxyl (alkoxy) substituents, which condense during cure to give a three-dimensional, cross-linked network. The MSSQ does not decompose at temperatures below  $500^\circ\text{C}$  in an inert atmosphere and has relatively low film stress. The dielectric constant of MSSQ ranges from 2.7 to 2.9, which is substantially lower than that of  $\text{SiO}_2$ ,  $\sim 4$ .<sup>5</sup> Making the MSSQ dielectric porous, lowers the dielectric constant further.

In this paper, we present the results on the dielectric properties of nanoporous thin films prepared from compatible blends of MSSQ and poly(dimethylaminoethyl methacrylate-co-methyl methacrylate) (DMAEMA-MMA) porogens. We describe results on low-frequency measurements using metal-insulator semiconductor (MIS) capacitors. Because new IMD thin films are expected to operate in the microwave regime, we also characterize the dielectric properties up to 10 GHz using a recently developed, high-frequency dielectric characterization technique.<sup>6</sup>

## EXPERIMENTAL TECHNIQUES

### Material and Sample Preparation

Test structures for dielectric characterization were fabricated using standard, complementary metal-oxide semiconductor processing techniques. The details of the preparation of the porous thin film are the following. The MSSQ ( $M_w = 1,500$  g/mol) was a research sample prepared by Dow Corning (Midland, MI) and supplied as a solid powder. The sample contained relatively little  $\text{SiOH}$  (infrared (IR) analysis) because of the method of preparation.<sup>7</sup> It was readily soluble in a variety of common spinning solvents including 1-methoxy-2-propanol, 1-methoxy-2-acetoxyp propane (PGMEA), ethyl lactate, etc. Various MSSQ structures with the same elemental composition can result by modifying the reagent stoichiometries, reaction conditions, and processing parameters.<sup>8</sup> All solutions were prepared using electronics-grade PGMEA. The MSSQ was stored refrigerated as 30% (w/w) solutions in PGMEA. All solutions contain both DMAEMA-MMA porogen<sup>4</sup> and MSSQ at a total of 30% solids (w/w) in the solvent. The porogen loadings used in this study were 10%, 30%, and 50%. Typically, the porosity mirrors the volume fraction of the porogen in the absence of significant pore collapse. In the system studied here, the respective densities of DMAEMA-MMA and MSSQ are similar, so weight percent and volume percent are used interchangeably. The thin-film densities are measured by x-ray reflectivity.<sup>9</sup> The solutions were passed through a filter (0.20- $\mu\text{m}$  Acrodisc [USA] CR polytetrafluoroethylene syringe filter) and

spin-coated onto a substrate. The substrate was spun at 2,500 rpm for 30 sec and placed directly onto a  $50^\circ\text{C}$  hot plate under nitrogen to remove most of the solvent. The sample was then cured, under argon, from  $60^\circ\text{C}$  to  $450^\circ\text{C}$  at  $5^\circ\text{C}/\text{min}$  and held for 1 h before cooling. After heating at  $450^\circ\text{C}$  for 1 h, the porogen is eliminated (thermal gravimetric analysis indicates a maximum of 1–2% char), and the resin is largely cured (no change in the IR spectra upon continued heating at this temperature under nitrogen).

### Low-Frequency Dielectric Measurement

A multiprobe capacitance analyzer was built to characterize the dielectric permittivity in the frequency range 20 KHz to 1 MHz in an array of identical MIS capacitors fabricated on a Si wafer. The setup has a nitrogen-filled test chamber, a copper wafer holder, thermoelectric cooler, a temperature-controlling unit, and a multiprobe station fixture to probe individually 16 MIS capacitors fabricated on a silicon wafer. A high-precision impedance meter (HP4192A, from Hewlett Packard Inc., USA) is used to measure the capacitance of each MIS capacitor.

The dielectric constants of the porous thin films were calculated from the measured capacitance of a MIS capacitor. The dielectric layer is spin coated onto a p-doped silicon wafer (3 in.  $\times$  375 mm, single-side polished, boron doped to a resistivity of  $<0.005$   $\Omega$  cm). The top aluminum metal contact is vacuum deposited using a shadow mask. The A +1-V bias on the metal plate is applied to bias the MIS capacitor in the accumulation regime, which avoids the influence of bias voltage and substrate type. Two calibration capacitors, built into the multiprobe station, are used to measure the parasitic capacitances of the system and the LCR-meter connection cables. From the thickness, measured independently, and capacitance measurement of each capacitor, the dielectric constant of the thin film is calculated by averaging all these measured data to improve the measurement accuracy.

### High-Frequency Dielectric Measurement

In the microwave regime, we obtain the dielectric permittivity from propagation constant measurements on thin-film, parallel-plate transmission lines as described in more detail in Ref. 6. Sets of transmission lines are fabricated with the MSSQ thin films. The transmission lines have the same cross-sectional geometry, but they have different lengths. The propagation constant as a function of frequency is determined from reflection and transmission coefficient measurements on the transmission lines. The complex propagation constant of the transmission lines is measured as a function of frequency from 1 GHz to 10 GHz with a vector network analyzer (HP 8510B) and a microwave probe station (Cascade, [USA] with coplanar probes ACP40-GSG). With the propagation constant known, the dielectric constant and loss tangent of low-dielectric, porous thin films are extracted using a precise electromagnetic

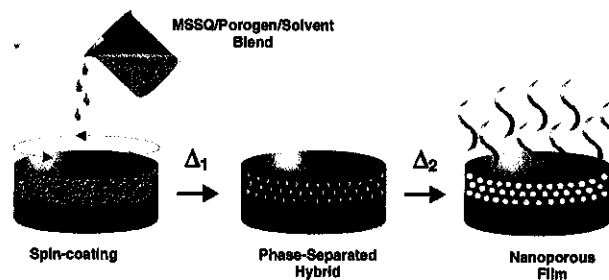
model that relates the propagation constant of the parallel-plate transmission line to the dielectric permittivity.

The test structure is built on a quartz substrate and contains two sets of parallel plates and one set of coplanar transmission-line structures. Each set of test structures has transmission lines of length 2 mm, 7 mm, 10 mm, 13 mm, 20 mm, and 29 mm. The purpose of multiple transmission-line lengths is to reduce the random measurement errors. Two identical sets of parallel-plate structures are used to further increase the redundancy. The coplanar transmission-line structures are used to measure the substrate dielectric constant. The bottom conducting plates of the parallel-plate transmission lines are embedded into the substrate by etching trenches into the substrate and controlling the deposition rate and thickness of the aluminum such that the resulting surface is as smooth as possible. This improves the uniformity and adhesion to the substrate and metal of the spin-coated film. The thickness of the parallel metal plates is about 2  $\mu\text{m}$  and chosen to reduce the evanescent waves at low frequencies. The bottom metal width is 40  $\mu\text{m}$ , which is chosen to minimize the fringing field effects in the parallel-plate structure. The top metal width is 500  $\mu\text{m}$  and serves as a shield to protect the dielectric thin film during the device fabrication procedure.

The scattering parameters are measured from 2 GHz to 10 GHz with a vector network analyzer (HP 8510B). The output power of the network analyzer at both ports is set to 10 dBm, and the attenuation is set to 0 dBm. A probe station is used for on-wafer testing (Cascade probe station with air coplanar probes ACP40-GSG). Systematic measurement errors are minimized by using the conventional thru-reflect-line (TRL) calibration algorithm.<sup>10</sup> The propagation constant is the parameter of interest and is calculated directly from uncalibrated, scattering-parameter measurements of two transmission lines by an adapted, TRL calibration algorithm.<sup>11</sup> Random errors are minimized by making multiple, redundant measurements and computing from a weighted average to give the noisy data less significance as described in Ref. 12.

## RESULTS AND DISCUSSION

Our general method of forming nanoporous MSSQ is outlined in Fig. 1. A solution containing the organic porogen and low molecular weight MSSQ is first spin coated onto a substrate. Upon thermally curing, the glass-resin MSSQ cross links initiating phase separation of the organic porogen into nanoscopic domains, where growth is restricted because of concomitant vitrification of the MSSQ. The organic polymer decomposes with increasing temperature, and the organic fragments diffuse out of the matrix to yield a porous material with a morphology nearly identical to that of the corresponding nanohybrid.



$\Delta_1$  = Solvent evaporation and nanohybrid formation (200 – 250 °C)

$\Delta_2$  = Porogen volatilization, porosity formation and MSSQ consolidation (350 – 450 °C)

Fig. 1. Processing steps necessary to generate nanoporosity in MSSQ.

A critical feature in this approach (nucleation and growth) is the initial compatibility of the organic porogen and the inorganic matrix material. As polymers are usually mutually insoluble, this requirement for compatibility requires some planning. For the matrix, we selected a SSQ prepolymer of MSSQ with a low molecular weight ( $M_n < 2,000$  g/mol), which assures the presence of polar chain ends. Because these MSSQ materials are prepared by acid hydrolysis, the chain ends are usually SiOH or SiOR moieties, and the resulting prepolymers are quite polar. Because polymer-polymer miscibility depends on the presence of strong interactions (ionic, hydrogen bonding, etc.), appropriate functionality must be introduced into the organic porogen. For polymers with weakly interacting backbone functionality, this can be accomplished by the introduction of polar chain ends. In an attempt to maximize the number of porogen chain ends, we initially studied multiarm stars, dendrimers, and hyperbranched materials. Controlled-ring opening and living free-radical techniques can be used to generate materials of this type with controlled molecular weights, low polydispersities, tailored functionality, and complex architectures. A six-arm star poly(caprolactone) (PCL), shown in Fig. 2, provides an early example of a macromolecular porogen, which was useful in MSSQ.<sup>13</sup> Here, the PCL arms are thermally stable to above the MSSQ vitrification temperature, but the porogen phase eventually separates into nanoscopic domains and decomposes to small molecules that diffuse from the film, producing well-defined pores. For weakly interacting polymer functionality, multiple polar-chain ends are useful for maintaining polymer-polymer compatibility until enough crosslinking has occurred in the matrix to assure the formation and maintenance of nanoscopic polymer domains. For PCL derivatives, which are chain hydrophobic, the polymer architecture can be important for the porous morphology. Figure 3 shows the porous morphologies (field-emission scanning electron microscopy) as a function of porogen architecture. In the pictures, the initial loading level was 20 wt.%, and the porogens were of comparable molecular weight. From these photomicrographs, we see that linear PCL is

immiscible and undergoes macroscopic phase separation producing huge pores. The size of the pores decreases with branching as evidenced by the porous morphologies generated for the six-arm star and the hyperbranched system.

If, on the other hand, the porogen polymer contains functional groups that strongly interact with the SSQ prepolymer (which in this study was MSSQ), even linear polymers can be employed. Examples of this category would be poly(alkylene ethers) and

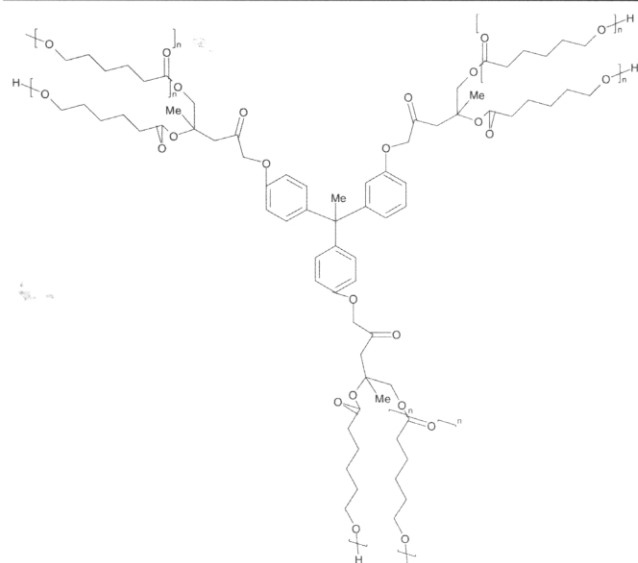
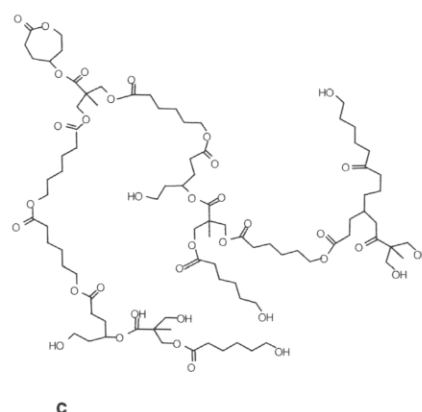
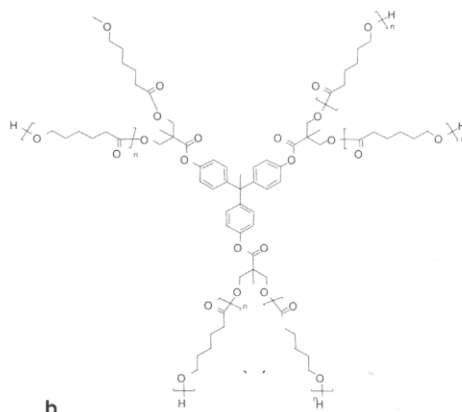
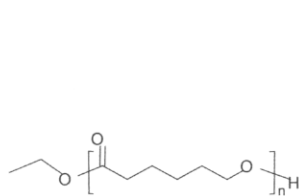
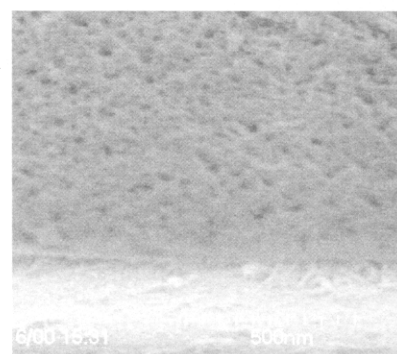
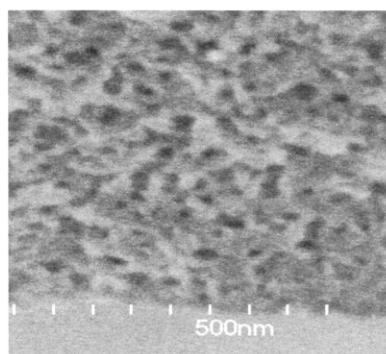
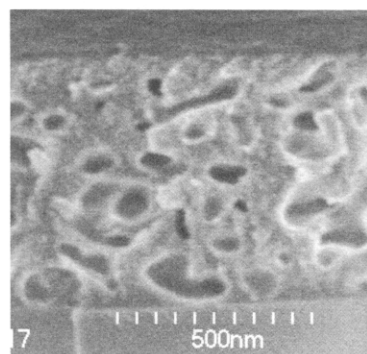


Fig. 2. Six-arm star PCL polymer.

methacrylate copolymers containing nitrogeous comonomers (e.g., vinyl pyridine, N,N-dimethyl acrylamide, N,N, dialkylaminoalkyl methacrylate, etc.). A useful example of the latter would be poly(DMAEMA-MMA). Interestingly, the presence of the basic alkylamino substituents as part of the polymer chain does not cause gellation when mixed with the SSQ prepolymers, although the hybrid formulations will exhibit increasing solution viscosities when stored at ambient temperatures. An added benefit of nitrogen-containing methacrylate copolymers is superb coatings are obtained upon spin coating the polymer mixture. For DMAEMA-MMA, the coating quality is optimized when the copolymer contains between 15% and 25% of the DMAEMA comonomer. In this study, we have chosen DMAEMA-co-MMA = 25/75 with molecular weights ( $M_w$ ) around 12,000 g/mol. The specific interactions of the dimethylamino substituents of the porogen with the SiOH end groups of the resin as determined by Fourier transform IR studies have been described elsewhere.<sup>4</sup> These strong interactions result in miscible blends with MSSQ resins over a composition range from 0% to 50% and higher. Over this range, pore dimensions, ranging from 2 nm to 10 nm, were determined by small angle x-ray scattering<sup>14</sup> and by transmission electron microscopy. The porous morphologies of these samples are consistent with a nucleation and growth mechanism and depend on porogen structure, loading level, molecular weight and polydispersity, resin structure, and processing conditions. The percolation threshold



a

b

c

Fig. 3. Porous MSSQ morphologies as a function of porogen molecular architecture: (a) linear, (b) six-arm star, and (c) hyperbranched.

of this system, as determined by positron annihilation spectroscopy, occurs around a loading level of 20 wt.%.<sup>15</sup>

As the porosity increases, substantial film shrinkage occurs at very high porogen loadings. Figure 4 shows the thickness and index of refraction ( $\lambda = 633$  nm) as a function of porosity. The refractive indices and film thicknesses were measured using a Filmetrics (U.K.) F20 spectral reflectometer. Above 60% porogen content, a sharp break occurs, which is attributed to the phase transition where the MSSQ becomes the dispersed phase. For this reason, we focus our attention on porogen content less than 60%.

The measured dielectric constants of 10%, 30%, and 50% porous MSSQ films are summarized in Table I and shown in Fig. 5 for measurements at 100 kHz and 10 GHz. The thicknesses of the films used in the high-frequency measurements were  $1.02 \pm 0.04$   $\mu\text{m}$  for 10% porosity,  $1.17 \pm 0.05$   $\mu\text{m}$  for 30% porosity, and  $0.61 \pm 0.05$   $\mu\text{m}$  for 50% porosity. The higher measurement error in the 50% porous-MSSQ samples is due to the larger uncertainty in the film thickness measurement. The dashed lines in Fig. 5 indicate the calculated dielectric constant for different polymer loading by the Bruggeman mixing relationship.<sup>16</sup> Within the measurement error, the measured values agree well with the calculated predictions. The dielectric constant of porous MSSQ at high frequencies agrees with its low-frequency value within experimental error, indicating small dispersion in the dielectric properties of the porous

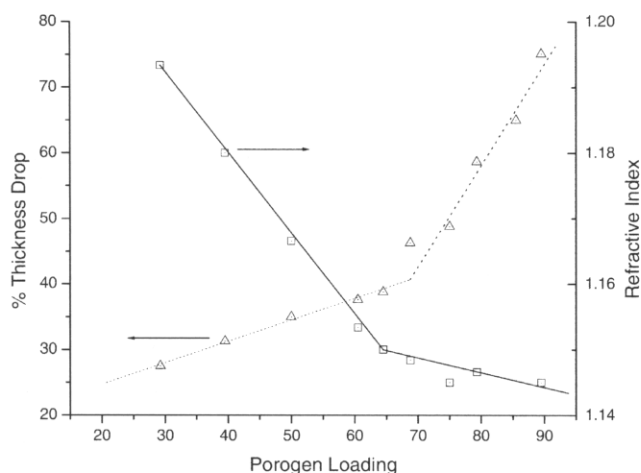


Fig. 4. Film shrinkage and refractive index as a function of porogen loading.

**Table I. Dielectric Constant of MSSQ with Different Porosities at Different Frequencies Measured at Room Temperature**

| Porosity | 100 KHz         | 2 GHz           | 10 GHz          |
|----------|-----------------|-----------------|-----------------|
| 10 pct   | $2.55 \pm 0.04$ | $2.43 \pm 0.20$ | $2.50 \pm 0.09$ |
| 30 pct   | $2.07 \pm 0.04$ | $2.11 \pm 0.16$ | $2.07 \pm 0.07$ |
| 50 pct   | $1.77 \pm 0.12$ | $1.92 \pm 0.25$ | $1.85 \pm 0.16$ |

MSSQ up to 10 GHz. This provides the first direct confirmation that the dielectric constant of the porous films behaves as expected up to at least 10 GHz, and in particular, there is no evidence of moisture absorption, which will lead to a drastic increase in the dielectric loss, in the films. The measured dielectric constants were unchanged after two weeks in laboratory ambient. The dielectric constants of the films measured at 100 kHz as a function of temperature are presented in Fig. 6. The changes in the dielectric constant in all cases are small and comparable, which indicates that the MSSQ host is providing a rigid, inorganic matrix. The measured dielectric constants for the three porosities in the 2 GHz to 10 GHz regime are shown in Fig. 7. Within the precision of the high-frequency measurement for dielectric loss tangents, which are less than 0.1, the loss tangent in all the films are small and, more importantly, showed no frequency dependence from 2 GHz to 10 GHz. If there was any

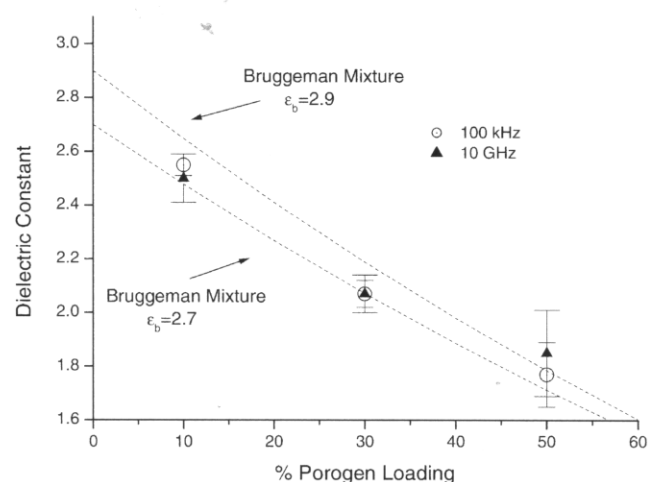


Fig. 5. Measured dielectric constant of porous MSSQ films at low frequency and in the microwave. The dashed lines are the calculated dielectric constant as a function of porogen loading.

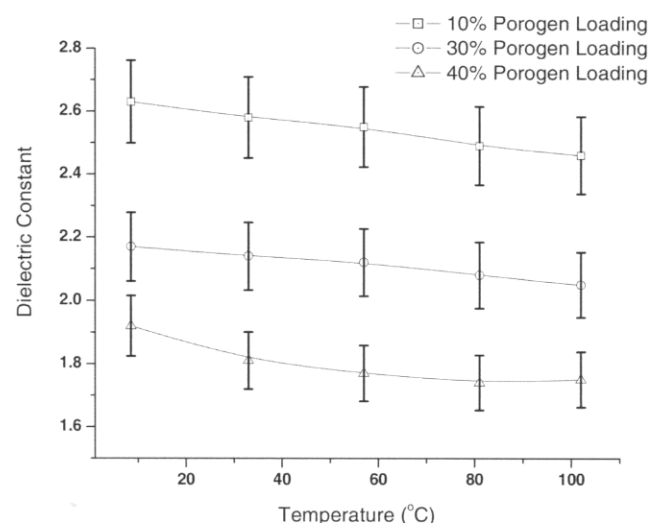


Fig. 6. Dielectric constants of porous MSSQ films measured at 100 kHz as a function of temperature.

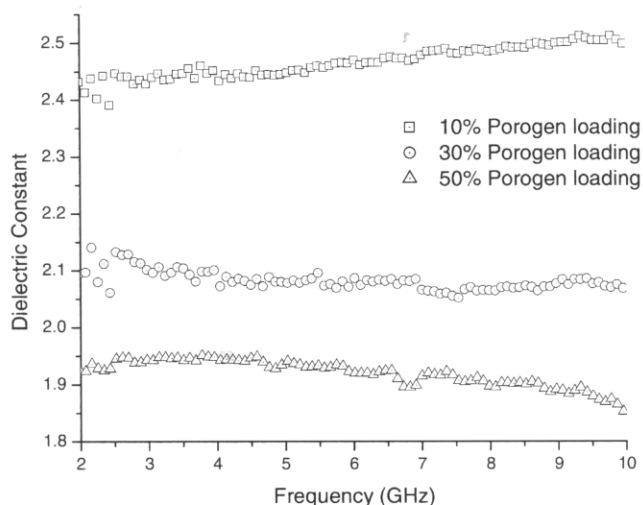


Fig. 7. Microwave measurements of the dielectric constant of MSSQ thin films with 10%, 30%, and 50% porogen loading, indicating that MSSQ is a low dielectric constant and low dispersion material at microwave regime.

water present in the films, it is expected that there would have been a large change in the loss tangent in this frequency regime.<sup>17</sup> This result confirms that the porous MSSQ films are very low loss materials in the microwave frequency range.

### CONCLUSIONS

We have studied the dielectric properties of thin, nanoporous films of MSSQ prepared using sacrificial, macromolecular pore generators. In this case, we used a copolymer of poly(DMAEMA-co-MMA) = 25/75 as a pore generator. The material strongly interacts with the SSQ matrix before curing to form miscible blends over a wide range of compositions. Porous material is generated by the thermal decomposition of the porogen. Although nanoscopic voids are produced over the range of compositions studied, it had been previously determined that percolation occurs in this system around void volumes of 20%.<sup>13</sup> The low-frequency dielectric constants of the film decrease with increasing porosity as expected. However, because modern devices will operate in the microwave range, the frequency dispersion, the dielectric constant, and losses at high frequencies are important and difficult to measure for thin constrained films. Using planar transmission-line

techniques developed in our laboratories, we have shown that there is little change in either the dielectric constant or loss measured up to 10 GHz. Because the loss measurements are particularly sensitive to the presence of water, we conclude that the intrinsic hydrophobic nature of MSSQ excludes water even at high porosities.

### ACKNOWLEDGEMENTS

This work was supported by the National Science Foundation MRSEC, Center on Polymer Interfaces and Macromolecular Assemblies, Contract No. DMR 9808677, and NIST Advanced Technology Program, Contract No. 70NANB8H4013.

### REFERENCES

1. D. Edelstein et al., *Technical Digest IEEE Int. Electron Devices Mtg.* (Piscataway, NJ: IEEE, 1997), pp. 773–776.
2. P. Singer, *Semicond. Int.* 21, 90 (1998).
3. R.H. Baney, M. Itoh, A. Sakakibara, and T. Suzuki, *Chem. Rev.* 95, 1409 (1995).
4. Q.R. Huang, W. Volksen, E. Huang, M. Toney, C.W. Frank, and R.D. Miller, *Chem. Mater.* 14, 3676 (2002).
5. J.L. Hedrick, R.D. Miller, C.J. Hawker, K.R. Carter, W. Volksen, D.Y. Yoon, and M. Trollsas, *Adv. Mater.* 10, 1049 (1998).
6. G. Song, S. Follonier, A. Knoesen, and R.D. Miller, *IEEE Microwave Guided Wave Lett.* 10, 183 (2000).
7. (a) C.L. Frye and W.T. Collins, *J. Am. Chem. Soc.* 92, 5586 (1970). (b) W.T. Collins and C.L. Frye, U.S. patent 3,615,272 (26 October 1971).
8. L.-H. Lee, W.-C. Chen, and W.-C. Liu, *J. Polym. Sci.: Part A: Polym. Chem.* 40, 1560 (2002).
9. M.F. Toney and S. Brennan, *J. Appl. Phys.* 64, 1861 (1989).
10. G.F. Engen and C.A. Hoer, *IEEE Trans. Microwave Theory Tech.* 27, 987 (1979).
11. M.D. Janezic and J.A. Jargon, *IEEE Microwave Guided Wave Lett.* 9, 76 (1999).
12. R.B. Marks, *IEEE Trans. Microwave Theory Tech.* 39, 1205 (1991).
13. (a) C.V. Nguyen et al., *Chem. Mater.* 11, 3080 (1999). (b) J.F. Remenar, C.J. Hawker, J.L. Hedrick, S.M. Kim, R.D. Miller, C. Nguyen, M. Trollsas, and D.G. Yoon, *Proc. Mater. Res. Soc.* 511, 69 (1998). (c) R.D. Miller et al., *Mater. Res. Soc. Symp. Proc.* 565, 3 (1999).
14. E. Huang et al., *Appl. Phys. Lett.* 81, 2232 (2002).
15. K.P. Rodbell, M. Petkov, M.H. Weber, K.G. Lynn, W. Volksen, and R.D. Miller, *Mater. Sci. Forum* 15, 363 (2001).
16. V.D.A.G. Bruggeman, *Annalen der Physik* 24, 636 (1935).
17. (a) L.W. Hrubesh, L.E. Keene, and V.R. Latorre, *J. Mater. Res.* 8, 1736 (1993). (b) L.W. Hrubesh and S.R. Buckley, *Low-Dielectric Constant Materials III Symp.* (Pittsburgh, PA: Materials Research Society, 1997), pp. 99–104.